

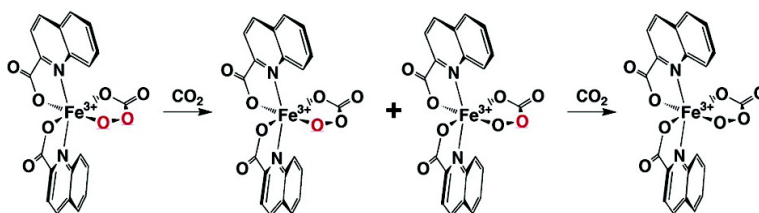
Communication

Reversible O–O Bond Cleavage and Formation of a Peroxo Moiety of a Peroxocarbonate Ligand Mediated by an Iron(III) Complex

Hideki Furutachi, Koji Hashimoto, Shigenori Nagatomo, Taichi Endo, Shuhei Fujinami, Yoshihito Watanabe, Teizo Kitagawa, and Masatatsu Suzuki

J. Am. Chem. Soc., **2005**, 127 (13), 4550-4551 • DOI: 10.1021/ja0427202 • Publication Date (Web): 10 March 2005

Downloaded from <http://pubs.acs.org> on March 25, 2009



More About This Article

Additional resources and features associated with this article are available within the HTML version:

- Supporting Information
- Links to the 3 articles that cite this article, as of the time of this article download
- Access to high resolution figures
- Links to articles and content related to this article
- Copyright permission to reproduce figures and/or text from this article

[View the Full Text HTML](#)



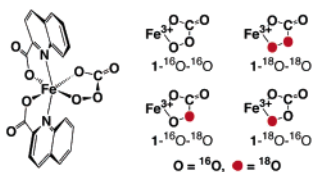
Reversible O–O Bond Cleavage and Formation of a Peroxo Moiety of a Peroxocarbonate Ligand Mediated by an Iron(III) Complex

Hideki Furutachi,[†] Koji Hashimoto,[†] Shigenori Nagatomo,[‡] Taichi Endo,[†] Shuhei Fujinami,[†] Yoshihito Watanabe,[§] Teizo Kitagawa,[‡] and Masatatsu Suzuki^{*†}

Department of Chemistry, Faculty of Science, Kanazawa University, Kakuma-machi, Kanazawa 920-1192, Japan, Center for Integrative Bioscience, Okazaki National Research Institutes, Myodaiji, Okazaki, 444-8585, Japan, and Department of Chemistry, Graduate School of Science, Nagoya University, Chikusa-ku, Nagoya 464-8602, Japan

Received December 3, 2004; E-mail: suzuki@cacheibm.s.kanazawa-u.ac.jp

Mononuclear iron complexes having a peroxo group such as η^2 -peroxide, η^1 -hydroperoxide, alkylperoxide, or peroxocarbonate are of particular importance for understanding the reaction mechanisms in various oxidation reactions catalyzed by mononuclear iron enzymes and their functional models.^{1,2} The O–O bond cleavage of the peroxo group is a key step of dioxygen activation by metal complexes. On the other hand, the O–O bond formation is also essential for the dioxygen formation by water oxidation. Reversible O–O bond cleavage and formation were first observed in the equilibrium between $(\mu-\eta^2:\eta^2\text{-peroxo})\text{Cu(II)}_2$ and $\text{bis}(\mu\text{-oxo})\text{Cu(III)}_2$ complexes by Tolman and co-workers³ and more recently by others.⁴ Recently, reversible O–X bond formation between Fe(IV)– or Mn(V)–(oxo)(porphyrin) complexes and X (X = Cl[–], Br[–], PhI) have also been reported.⁵ Herein we report the first example of reversible O–O bond cleavage and formation of a peroxo group involving an iron(III) complex containing a peroxocarbonate ligand, $[\text{Fe}(\text{qn})_2(\text{O}_2\text{C}(\text{O})\text{O})]^-$ (**1**) (qn = quinaldinate).²



Complex **1** is stable at -40°C in acetonitrile and DMF under CO_2 for weeks. The resonance Raman spectrum of $[\text{Fe}(\text{qn})_2(^{18}\text{O}-^{18}\text{O})\text{C}(\text{O})\text{O}]^-$ (**1**- $^{18}\text{O}-^{18}\text{O}$) in acetonitrile at -40°C shows a $\nu(\text{O}-\text{O})$ band at 842 cm^{-1} (Figure 1a). Upon warming the solution up to 20°C , we observed that drastic spectral changes occurred to give new bands at 858, 868, and 884 cm^{-1} (spectra b–d and c'). By comparing the authentic sample (**1**-scrambled) prepared from ^{18}O -labeled H_2O_2 ($\text{H}_2^{16}\text{O}_2/\text{H}_2^{16}\text{O}^{18}\text{O}/\text{H}_2^{18}\text{O}_2 = 25:50:25$), we assigned these bands to the $\nu(\text{O}-\text{O})$ vibrations of **1**- $^{18}\text{O}-^{16}\text{O}$, **1**- $^{16}\text{O}-^{18}\text{O}$, and **1**- $^{16}\text{O}-^{16}\text{O}$, respectively. These spectral changes clearly demonstrate the successive conversion from **1**- $^{18}\text{O}-^{18}\text{O}$ through **1**- $^{18}\text{O}-^{16}\text{O}$ and **1**- $^{16}\text{O}-^{18}\text{O}$ to **1**- $^{16}\text{O}-^{16}\text{O}$, where the intensity ratio of **1**- $^{18}\text{O}-^{16}\text{O}$ and **1**- $^{16}\text{O}-^{18}\text{O}$ is the same as that observed for **1**-scrambled (cf. spectra c' and e'), indicating that the formation rates of these two species are the same. The ESI-TOF/MS intensity changes of three isotopomers (**1**- $^{18}\text{O}-^{18}\text{O}$, **1**- $^{18}\text{O}-^{16}\text{O}$ + **1**- $^{16}\text{O}-^{18}\text{O}$, and **1**- $^{16}\text{O}-^{16}\text{O}$) in DMF at 20°C also showed the successive conversion from **1**- $^{18}\text{O}-^{18}\text{O}$ ($m/z = 480$) through **1**- $^{18}\text{O}-^{16}\text{O}$ + **1**- $^{16}\text{O}-^{18}\text{O}$ ($m/z = 478$) to **1**- $^{16}\text{O}-^{16}\text{O}$ ($m/z = 476$) together with the decomposition of **1** (Figure 2). In addition, the reverse

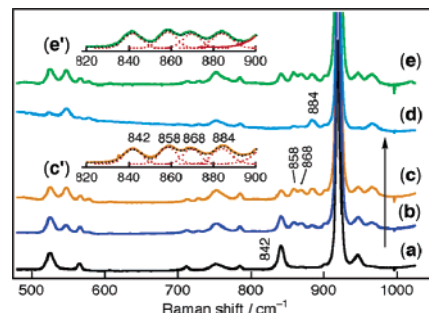


Figure 1. Raman spectra of **1**- $^{18}\text{O}-^{18}\text{O}$ (a) at -40°C , warming at 20°C (b) for 5 min, (c) for 10 min, (d) for 30 min, and (e) that of **1**-scrambled in acetonitrile at -40°C . Insets (c' and e') are Gaussian analyses of the $\nu(\text{O}-\text{O})$ bands of (c) and (e).

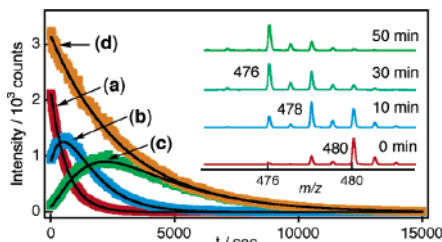


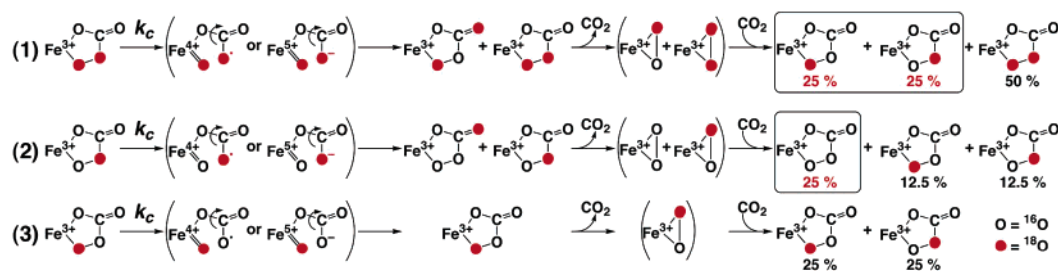
Figure 2. Time courses of ESI-TOF/MS intensity changes of **1** in DMF at 20°C under CO_2 (bubbling for 3 min). Conversion profiles of (a) **1**- $^{18}\text{O}-^{18}\text{O}$ ($m/z = 480$), (b) **1**- $^{18}\text{O}-^{16}\text{O}$ + **1**- $^{16}\text{O}-^{18}\text{O}$ ($m/z = 478$), (c) **1**- $^{16}\text{O}-^{16}\text{O}$ ($m/z = 476$), and (d) decomposition profile of **1**. Solid lines are the fitting curves using eqs 2–4 with $k_c = 2.4 \times 10^{-3}\text{ s}^{-1}$ and $k_d = 3.4 \times 10^{-4}\text{ s}^{-1}$. The inset is the ESI-TOF/MS spectral changes of **1** with time, where intensities of main signals are normalized for clarity.

conversion from $[\text{Fe}(\text{qn})_2(^{16}\text{O}-^{16}\text{O})\text{C}(\text{O})\text{O}]^-$ to $[\text{Fe}(\text{qn})_2(^{18}\text{O}-^{18}\text{O})\text{C}(\text{O})\text{O}]^-$ was observed by the reaction with C^{18}O_2 (Figure S1), indicating that oxygens of the peroxo moiety come from C^{18}O_2 . It was also found that exchange of the CO_2 moiety ($\text{O}-\text{O}-\text{C}(=\text{O})\text{O}$) and isotope exchange of the O–O moiety ($\text{O}-\text{O}-\text{C}(=\text{O})\text{O}$) occur independently, and the former is much faster than the latter, and this was confirmed by the reactions with $^{13}\text{CO}_2$ and C^{18}O_2 by ESI-TOF/MS spectroscopy (Figures S1 and S2). The results indicate that, unlike $[\text{RhCl}(\text{O}-\text{O}-\text{C}(\text{O})\text{O})(\text{PET}_2\text{Ph})_3]$,⁶ formation of peroxocarbonate in **1** does not involve O–O bond cleavage of the peroxide and there is a rapid equilibrium between **1** and $[\text{Fe}(\text{qn})_2(\text{O}_2)]^-$ (eq 1). Although $[\text{Fe}(\text{qn})_2(\text{O}_2)]^-$ has not been detected at present, side-on peroxo–iron(III) species have been well-established.^{1g,7}



The decomposition rate of **1** is highly dependent on the reaction conditions such as concentrations of CO_2 and H_2O (vide infra),

[†] Kanazawa University.
[‡] Okazaki National Research Institutes.
[§] Nagoya University.

Scheme 1. Possible Conversion Pathways from $1\text{-}^{18}\text{O}\text{-}^{18}\text{O}$ through $1\text{-}^{18}\text{O}\text{-}^{16}\text{O}$ and $1\text{-}^{16}\text{O}\text{-}^{18}\text{O}$ to $1\text{-}^{16}\text{O}\text{-}^{16}\text{O}$ 

but the conversion profiles shown in Figure 2 are not significantly affected (Figures S3 and S4), suggesting that CO_2 and H_2O are not involved in the rate-determining step (vide infra). Possible conversion pathways are shown in Scheme 1. The first step is O–O bond cleavage of the peroxy moiety to generate a high-valent $\text{Fe}^{\text{IV}}=\text{O}$ or $\text{Fe}^{\text{V}}=\text{O}$ species as found for $\text{M}(\text{III})(\text{peroxocarbonato})(\text{porphyrin})$ ($\text{M} = \text{Mn}$ and Fe),⁸ which is assumed to be a rate-determining step in the conversion processes. Although such high-valent iron-oxo species have not been detected in this study, $\text{Fe}^{\text{IV}}=\text{O}$ species have been well-established.^{15,9} Rotation around the O–C bond ($\text{O}=\text{Fe}-\text{O}-\text{C}(\text{O})\text{O}$) and reformation of the O–O bond produce $1\text{-}^{18}\text{O}\text{-}^{18}\text{O}$ and $1\text{-}^{18}\text{O}\text{-}^{16}\text{O}$ in a 1:1 ratio. Then rapid equilibrium with $1\text{-}^{18}\text{O}\text{-}^{16}\text{O}$ and CO_2 generates $1\text{-}^{18}\text{O}\text{-}^{16}\text{O}$ (25%) and $1\text{-}^{16}\text{O}\text{-}^{18}\text{O}$ (25%), where the overall conversion to $1\text{-}^{18}\text{O}\text{-}^{16}\text{O}$ and $1\text{-}^{16}\text{O}\text{-}^{18}\text{O}$ is 50% based on $1\text{-}^{18}\text{O}\text{-}^{18}\text{O}$ (step 1 in Scheme 1). Conversion to $1\text{-}^{16}\text{O}\text{-}^{16}\text{O}$ occurs only from $1\text{-}^{16}\text{O}\text{-}^{18}\text{O}$ (step 2), but not from $1\text{-}^{18}\text{O}\text{-}^{16}\text{O}$ (step 3), where the conversion from ($1\text{-}^{18}\text{O}\text{-}^{16}\text{O} + 1\text{-}^{16}\text{O}\text{-}^{18}\text{O}$) to $1\text{-}^{16}\text{O}\text{-}^{16}\text{O}$ is 25%. This proposed mechanism yields the following rate equations including the decomposition of **1**.

$$d[\mathbf{A}]/dt = -(k_c/2 + k_d)[\mathbf{A}] \quad (2)$$

$$d[\mathbf{B}]/dt = (k_c/2)[\mathbf{A}] - (k_c/4 + k_d)[\mathbf{B}] \quad (3)$$

$$d[\mathbf{C}]/dt = (k_c/4)[\mathbf{B}] - k_d[\mathbf{C}] \quad (4)$$

where k_c and k_d are the first-order rate constants for the O–O bond cleavage and the decomposition of **1**, respectively, $\mathbf{A} = 1\text{-}^{18}\text{O}\text{-}^{18}\text{O}$, $\mathbf{B} = (1\text{-}^{18}\text{O}\text{-}^{16}\text{O} + 1\text{-}^{16}\text{O}\text{-}^{18}\text{O})$, $\mathbf{C} = 1\text{-}^{16}\text{O}\text{-}^{16}\text{O}$. The conversion profiles of the above three isotopomers and decay of **1** can be reasonably fitted with $k_c = 2.4 \times 10^{-3} \text{ s}^{-1}$ and $k_d = 3.4 \times 10^{-4} \text{ s}^{-1}$ as shown in Figure 2 (solid lines).¹⁰ In this mechanism, there is a possibility of direct exchange of the oxo group of putative $\text{Fe}^{\text{IV}}=\text{O}$ or $\text{Fe}^{\text{V}}=\text{O}$ species with water.^{9b} However, addition of water (500 equiv) causes no change in the conversion rate ($k_c = 2.2 \times 10^{-3} \text{ s}^{-1}$), although the decomposition rate is much accelerated ($k_d = 1.4 \times 10^{-3} \text{ s}^{-1}$, see Figure S3). The same is true for the CO_2 concentration effect (see Figure S4).¹¹ Thus the results indicate that a direct exchange of the oxo group of putative $\text{Fe}^{\text{IV}}=\text{O}$ or $\text{Fe}^{\text{V}}=\text{O}$ species is not significant and the oxygens of the peroxy group come from the oxygens of CO_2 (see also Figure S1).

In summary, we have succeeded in the first observation of the reversible O–O bond cleavage and reformation of the peroxy group via the formation of a high-valent iron-oxo species such as $\text{Fe}^{\text{IV}}=\text{O}$ or $\text{Fe}^{\text{V}}=\text{O}$, which binds its counterpart, carbonate radical or carbonate, in close proximity. This proximity effect may be responsible for the reformation of the O–O bond.

Acknowledgment. Financial support of this research by the Ministry of Education, Science, and Culture Grant-in-Aid for Scientific Research to H.F., M.S., T.K., and Y.W. is gratefully acknowledged.

Supporting Information Available: Experimental details of the kinetic studies and Figures S1–S5. This material is available free of charge via the Internet at <http://pubs.acs.org>.

References

- (1) See, for example: (a) Feig, A. L.; Lippard, S. J. *Chem. Rev.* **1994**, *94*, 759–805. (b) Que, L., Jr.; Ho, R. Y. N. *Chem. Rev.* **1996**, *96*, 2607–2624. (c) Girerd, J. J.; Banse, F.; Simaan, A. J. *Struct. Bonding* **2000**, *97*, 145–177. (d) Solomon, E. I.; Brunold, T. C.; Davis, M. I.; Kemsley, J. N.; Lee, S.-K.; Lehnert, N.; Neese, F.; Skulan, A. J.; Yang, Y.-S.; Zhou, J. *Chem. Rev.* **2000**, *100*, 235–349. (e) Solomon, E. I. *Inorg. Chem.* **2001**, *40*, 3656–3669. (f) Chen, K.; Costas, M.; Que, L., Jr. *J. Chem. Soc., Dalton Trans.* **2002**, 672–679. (g) Costas, M.; Mehn, M. P.; Jensen, M. P.; Que, L., Jr. *Chem. Rev.* **2004**, *104*, 939–986.
- (2) Hashimoto, K.; Nagatomo, S.; Fujinami, S.; Furutachi, H.; Ogo, S.; Suzuki, M.; Uehara, A.; Maeda, Y.; Watanabe, Y.; Kitagawa, T. *Angew. Chem., Int. Ed.* **2002**, *41*, 1202–1205.
- (3) (a) Halfen, J. A.; Mahapatra, S.; Wilkinson, E. C.; Kaderli, S.; Young, V. G., Jr.; Que, L., Jr.; Zuberbühler, A. D.; Tolman, W. B. *Science* **1996**, *271*, 1397–1400. (b) Tolman, W. B. *Acc. Chem. Res.* **1997**, *30*, 227–237. (c) Cahoy, J.; Holland, P. L.; Tolman, W. B. *Inorg. Chem.* **1999**, *38*, 2161–2168.
- (4) (a) Hayashi, H.; Fujinami, S.; Nagatomo, S.; Ogo, S.; Suzuki, M.; Uehara, A.; Watanabe, Y.; Kitagawa, T. *J. Am. Chem. Soc.* **2000**, *122*, 2124–2125. (b) Mirica, L. M.; Ottenwaelter, X.; Stack, T. D. P. *Chem. Rev.* **2004**, *104*, 1013–1045. (c) Hatcher, L. Q.; Karlin, K. D. *J. Biol. Inorg. Chem.* **2004**, *9*, 669–683.
- (5) (a) Nam, W.; Choi, S. K.; Lim, M. H.; Rohde, J.-U.; Kim, I.; Kim, J.; Kim, C.; Que, L., Jr. *Angew. Chem., Int. Ed.* **2003**, *42*, 109–111. (b) Jin, N.; Bourassa, J. L.; Tizio, S. C.; Groves, J. T. *Angew. Chem., Int. Ed.* **2000**, *39*, 3849–3851. (c) Wagenknecht, H.-A.; Woggon, W.-D. *Angew. Chem., Int. Ed.* **1997**, *36*, 390–392.
- (6) Aresta, M.; Tommasi, I.; Quaranta, E.; Fragale, C.; Mascetti, J.; Tranquille, M.; Galan, F.; Fouassier, M. *Inorg. Chem.* **1996**, *35*, 4254–4260.
- (7) Either side-on or end-on peroxy species is possible, although only side-on species have been well-established. See, for example: (a) Neese, F.; Solomon, E. I. *J. Am. Chem. Soc.* **1998**, *120*, 12829–12848. (b) Karlsson, A.; Parales, J. V.; Parales, R. E.; Gibson, D. T.; Eklund, H.; Ramaswamy, S. *Science* **2003**, *299*, 1039–1042.
- (8) (a) Weiss, R.; Schappacher, M. *Inorg. Chem.* **1987**, *26*, 1189–1190. (b) Schappacher, M.; Weiss, R.; Montiel-Montoya, R.; Trautwein, A.; Tabard, A. *J. Am. Chem. Soc.* **1985**, *107*, 3736–3738.
- (9) See, for example: (a) Rohde, J.-U.; In, J.-H.; Lim, M. H.; Brennessel, W. W.; Bukowski, M. R.; Stubna, A.; Münck, E.; Nam, W.; Que, L., Jr. *Science* **2003**, *299*, 1037–1039. (b) Seo, S. K.; In, J.-H.; Kim, S. O.; Oh, N. Y.; Hong, J.; Kim, J.; Que, L., Jr.; Nam, W. *Angew. Chem., Int. Ed.* **2004**, *43*, 2417–2420.
- (10) This k_d value is slightly larger than that obtained from the UV–vis measurements ($k_d = 2.6 \times 10^{-4} \text{ s}^{-1}$). This is due to the change in the reaction conditions; for ESI-TOF/MS experiments, a slightly lower CO_2 concentration was employed to suppress the occasional foaming of CO_2 .
- (11) In the absence of CO_2 , the decomposition is significantly accelerated; $k_d = 1.4 \times 10^{-2} \text{ s}^{-1}$ under N_2 and $k_d = 2.6 \times 10^{-4} \text{ s}^{-1}$ under CO_2 were obtained from the UV–vis measurements (see Figure S5).

JA0427202